REPORT DOCUMENTATION PAGE

AFRL-SR-AR-TR-02-

0177

1. REPORT DATE *(DD-MM-YYYY)* 01-05-2002	2. REPORT TYPE Final		3. DATES COVERED *(From - To)* 01-06-1998 31-05-2001
4. TITLE AND SUBTITLE Closed Loop Control of Advanced Manfuacturing Processes			**5a. CONTRACT NUMBER**
			5b. GRANT NUMBER F49620-98-1-0454
			5c. PROGRAM ELEMENT NUMBER
6. AUTHOR(S) P.F. Williams and N.J. Ianno			**5d. PROJECT NUMBER**
			5e. TASK NUMBER
			5f. WORK UNIT NUMBER
7. PERFORMING ORGANIZATION NAME(S) AND ADDRESS(ES) University of Nebraska-Lincoln 303 Admin Bldg. Lincoln, NE 68588-0430			**8. PERFORMING ORGANIZATION REPORT NUMBER** PFW-05-01-02
9. SPONSORING / MONITORING AGENCY NAME(S) AND ADDRESS(ES) AFOSR/NE 801 N. Randolph St. Arlington, VA 22203			**10. SPONSOR/MONITOR'S ACRONYM(S)**
			11. SPONSOR/MONITOR'S REPORT NUMBER(S)

12. DISTRIBUTION / AVAILABILITY STATEMENT

13. SUPPLEMENTARY NOTES

14. ABSTRACT
This report describes the results from a research effort investigating two candidate techniques for producing glow-like discharges in atmosphereic-pressure gases. The first techniques uses a mid-discharge constriction to avoid the formation of current filaments, whereas the second uses a plasma cathode produced by a hollow-cathode-like discharge.

20020614 164

15. SUBJECT TERMS
glow discharge atmospheric pressure

16. SECURITY CLASSIFICATION OF:			17. LIMITATION OF ABSTRACT	18. NUMBER	19a. NAME OF RESPONSIBLE PERSON P.F. Williams
a. REPORT unclassified	**b. ABSTRACT** unclassified	**c. THIS PAGE** unclassified	UL	18	**19b. TELEPHONE NUMBER** *(include area code)* (402)472-1970

Standard Form 298 (Rev. 8-98)
Prescribed by ANSI Std. Z39.18

FINAL REPORT
Advanced Diagnostics for Closed-Loop Process Control in Semiconductor Manufacturing

Grant F49620-98-0454

Covering the period June 1, 1998 to May 31, 2001

P.F. Williams and N.J. Ianno
Department of Electrical Engineering
University of Nebraska-Lincoln
Lincoln, NE 68588-0511

ABSTRACT

This report describes the results from a research effort investigating two candidate techniques for producing glow-like discharges in atmospheric-pressure gases. The first technique uses a mid-discharge constriction to avoid the formation of current filaments, whereas the second uses a plasma cathode produced by a hollow-cathode-like discharge.

1 INTRODUCTION

The goal of this project was to study atmospheric-pressure glow discharges. Two schemes for the production of such discharges were investigated: 1) a mid-discharge constriction such as reported by Kunhardt, and 2) a micro-hollow-cathode discharge such as discussed by Schoenbach *et al.*[1] [2] [3], and Frame *et al.*[4]. Our intent was to use plasma etching to produce dense arrays, "sieves," of 10 μm-diameter holes, in silicon and perhaps quartz wafers. A substantial portion of our effort was expended on developing the capability for fabricating these etched arrays.

This report is divided into three sections. The first describes the development of the etching technology, the second discusses empirical results with the micro-hollow-discharge configuration, and the third discusses results with the mid-discharge constriction configuration.

2 SIEVE FABRICATION

The goal of this section of the work was to fabricate "sieves" consisting of an array of holes roughly 10 μm in diameter in silicon wafers. The general plan involved the use of a TCP plasma reactor with CF_4 feedgas to etch the holes. A high-density plasma reactor, such as a TCP system, was required because of the requirement for etching holes 100 μm deep. An aluminum etch mask was used. Photolithography, coupled with a wet-chemical etch was used to form the hole pattern in the mask.

2.1 TCP Reactor Design and Characterization

At the start of the project, a TCP reactor was not available, making it necessary to design, construct, and characterize one. Additionally, we had not had experience with etching such deep features, and significant effort was required to develop our ability to do so.

Fig. 1 shows a schematic diagram of the system we designed. The main reactor chamber is made from an MDC base well modified to have four 2-3/4" and four 6" flanges on the side. Two of the 6" flanges were used to provide optical access to the chamber. In order to reduce etching of the windows, 10" long nipples were used as spacers. The chamber was evacuated with a Leyboldt 600C chemical-resistant, 600 l/sec turbomolecular pump.

A specially designed top plate was used to introduce the R.F. excitation. Fig. 2 shows a schematic diagram of the top plate. A 6" dia., 3/8" thick, O-ring sealed, fused quartz plate was used to introduce the R.F. into the chamber. A water-cooled "pancake" coil with about 1 1/2 turns was used as the primary winding of the TCP transformer. The coil was made of 1/4" copper tubing. One end of the coil was connected directly to the top plate, and the other to the output of a matching network. The top plate was O-ring sealed to the base well.

The sample to be etched was mounted on a water-cooled copper plate which was mounted on a translation feedthrough. The vertical position of the copper plate could be adjusted, but was generally placed about 3" below the primary TCP pancake coil. We wished to be able to bias the sample using a 13.6 MHz generator. For this reason, the support rod that connects
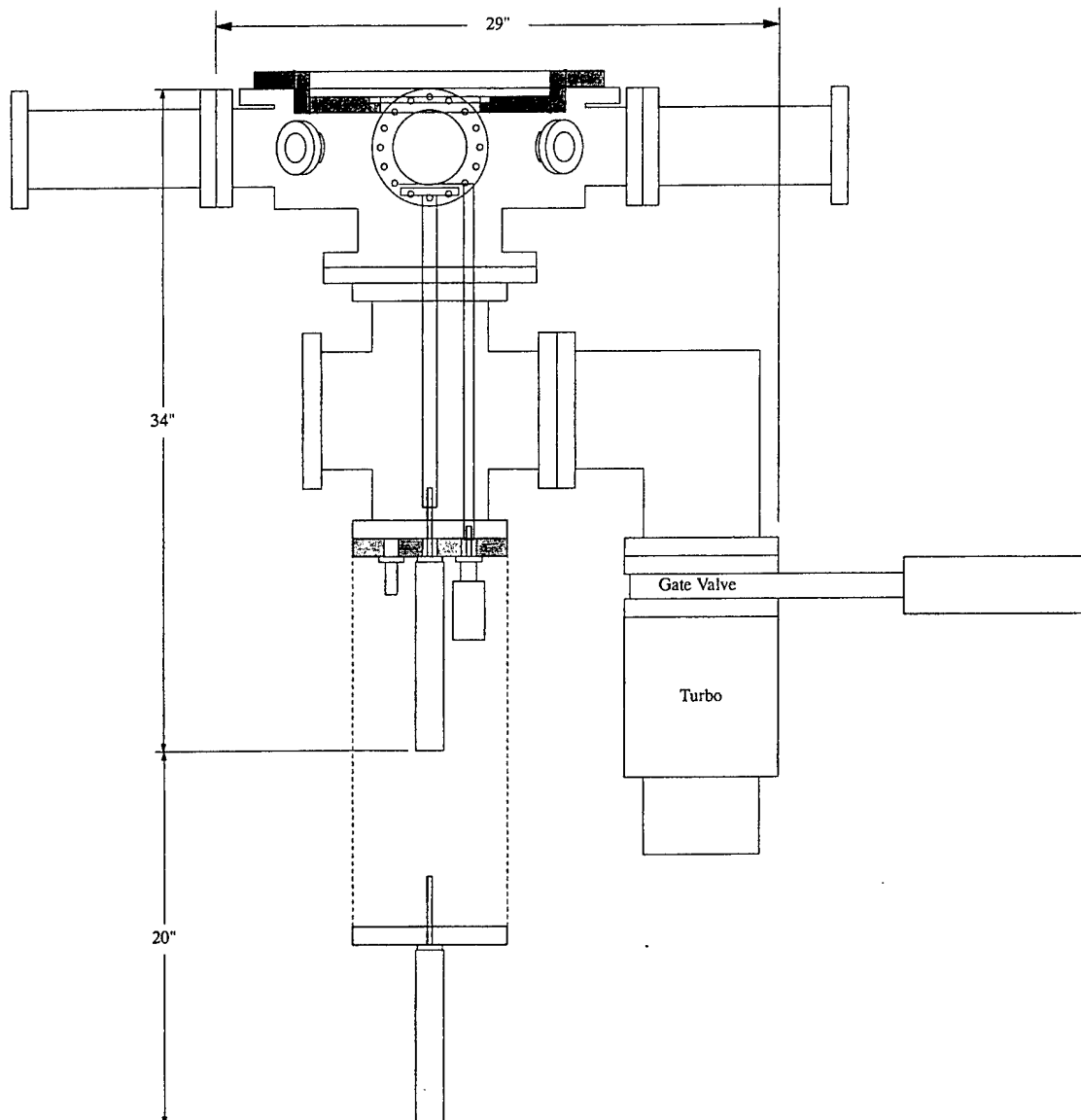
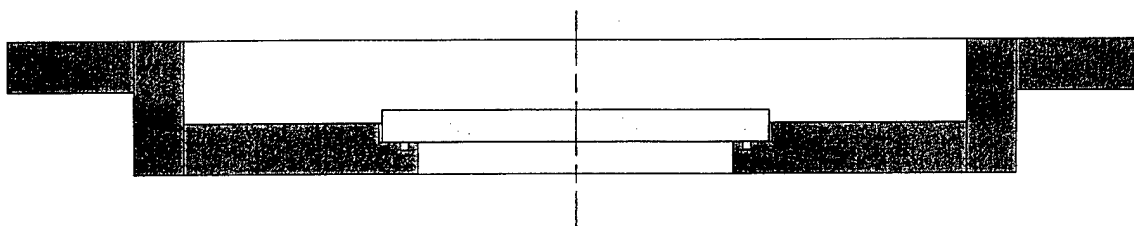**Figure 1:** Schematic diagram of TCP reactor vacuum chamber.

Figure 2: Schematic diagram of the top plate used in the TCP reactor. The shaded region is stainless steel.

mechanically the plate to the translation unit was insulated from ground by placing an ≈ 10 cm length of pyrex rod in the support. R.F. power was supplied to the plate using a length of rigid coaxial transmission line insulated using a pyrex tube between the inner and outer conductors. The final connection between the rigid coax and the plate was accomplished with a strip of copper foil about 0.5 cm wide.

The plate was water cooled by soldering several turns of 1/4" copper tubing to the underside. Water was supplied through teflon tubing coiled around the support rod. A Neslab chiller was used to supply deionized water at $25°$ C.

The bottom flange of the cell contained the water and R.F. feedthroughs as well as the linear translation feedthrough for adjusting the vertical position of the plate and a rotary feedthrough for "opening" and "closing" a shutter over the sample. To facilitate loading and unloading the reactor, the Conflat flange was sealed to the chamber with a neophrene, rather than copper, gasket. Three 1/4" case-hardened steel drill rods were used as guides to maintain alignment of the sample plate support rod with the axis of the chamber during insertion and removal. The bottom flange was attached to a bearing spider for this purpose. With this arrangement sample access was relatively convenient.

The main R.F. power for the TCP reactor was supplied through a "pancake" coil consisting of about 1 1/2 turns of 1/4" copper tubing. An Advanced Energy Systems AZX-90 matching network was used to match the generator output to the impedance of the discharge. Initially, power was supplied by an Advanced Energy Systems RFX 1250 solid-state generator. The protection circuitry in the solid-state generator caused problems when the discharge made the transition from capacitively-coupled to inductively-coupled modes. For this reason, we switched to using an old vacuum tube generator. Both generators operated at 13.56 MHz, and were capable of more than 1 KW of output power. The matching network and the "pancake" coil were water-cooled.

For initial testing and tuning of the reactor we used N_2. We found that the power threshold for the transition from the capacitive to the inductive coupling mode could be reduced from about 250 W to about 50 W in N_2 by adjusting the number of turns in the pancake coil. In the final configuration, the coil had about 1 1/2 turns. With the CF_4 fill we used for etching, this power threshold increased to about 200 W.

2.2 Plasma Etching

For etching silicon we used about a 10:1 ratio of CF_4/O_2. The purpose of the O_2 is to improve the etch rate. It is believed that it does so by reducing the deposition of CF polymers on the etched surface[5]. We measured the etch rate in our system as a function of several parameters. The measurement was made by using a drop of silver paint as a crude mask on a silicon wafer, etching for a set time. After removing the sample from the system, the silver paint was dissolved, and the height of the step between the masked and unmasked portions of the silicon was measured using a mechanical stylus.

We found that the etch rate increased with TCP power up to about 750 W. For 18 sccm CF_4 and 2 sccm O_2, the etch rate with 225 W was about 0.55 μm/min, and at 750 W, it was

about 1.2 μm/min. At 1000 W, the etch rate was essentially the same, 1.0 μm/min. We also explored the variation in etch rate with etchant flow rate. We found that with 750 W the etch rate increased to about 1.4 μm/min with 27 sccm CF_4 and 3 sccm O_2. This flow rate tended to overload the turbomolecular pump, however. For this reason, we generally used 18/2 sccm CF_4/O_2 flow.

Our plan was to use an Al film for an etch mask when we fabricated the sieve. For this reason, the etch rate of Al in our system was also important. Al films were deposited on silicon wafers using sputtering in Ar. Etch rates of the aluminum were measured in the same way that the etch rates of silicon were measured. Under the same conditions that we planned to use for etching silicon, we found the etch rate of Al to be $0.01 - 0.02$ μm/min. Our plan was to use silicon wafers 100 μm thick. In order to etch through the wafers without etching through the Al mask, the mask should be at least 2 μm thick. In making our sieves, we used 4 μm thick masks.

In order to fabricate the Al etch mask, photolithography was used. We used Olin Hunt RES IC type-3 negative photoresist which was spun onto the Al film and then baked at 85° C. A commercial photolithography contact mask was used to produce the desired pattern in the photoresist. The mask had an array of 10 μm diameter opaque dots with 100 μm spacing. The pattern was contained within a 1 cm circle, and the mask also had a 1 cm diameter , 200 μm thick circle on the boundary so that the etching process also cuts the sieve out of the wafer. After exposing and developing the photoresist, it was baked at 120° C. The bare aluminum was wet etched using a mixture of H_3PO_4, CH_3COOH, and HNO_3.

For testing the etching process, we used wafers about 300 μm thick. The reasons were that we had a large supply of such wafers available, the thicker wafers were easier to handle without breakage, and the thicker wafers allowed us to view the bottom of the etched well as well as the walls.

Fig. 3 shows an SEM photomicrograph of the pattern etched into such a silicon wafer. The pattern shows good uniformity, and the etch line delineating the 1 cm circle is also clearly seen. Fig. 4 shows a close-up top view of the holes we produced.

The hole has a slightly conical profile. The diameter of the top of the hole is about 26 μm, a bit more than twice the diameter of the hole in the aluminum etch mask. Thus it appears that the etch process must have an isotropic component, causing undercutting of the etch mask. Fig. 5 shows that this is indeed the case. It shows a cross-sectional SEM photomicrograph of a hole. The aluminum mask has not been stripped off, and it and the etch mask hole are visible at the top. As expected, the hole in the aluminum is 10 μm in diameter. The silicon just under the hole has been etched out under the aluminum to a diameter of about 25 μm. The etch time was 60 minutes.

The average longitudinal etch rate in this case was about 0.7 μm/min. This rate is somewhat smaller than the rate we measured in our initial tests. In the initial tests, the etched surface was not confined as it is here. The fact that the etch rate in the hole is about 60% of that in the unconstricted case implies that the etch rate in the hole is limited by transport of etchant to the etched surface or transport of the product out of the hole.

Fig. 6 shows a similar SEM photomicrograph, but this time for a total etch time of 135 minutes. The average longitudinal etch rate in this case decreased to about 0.6 μm/min. The di-
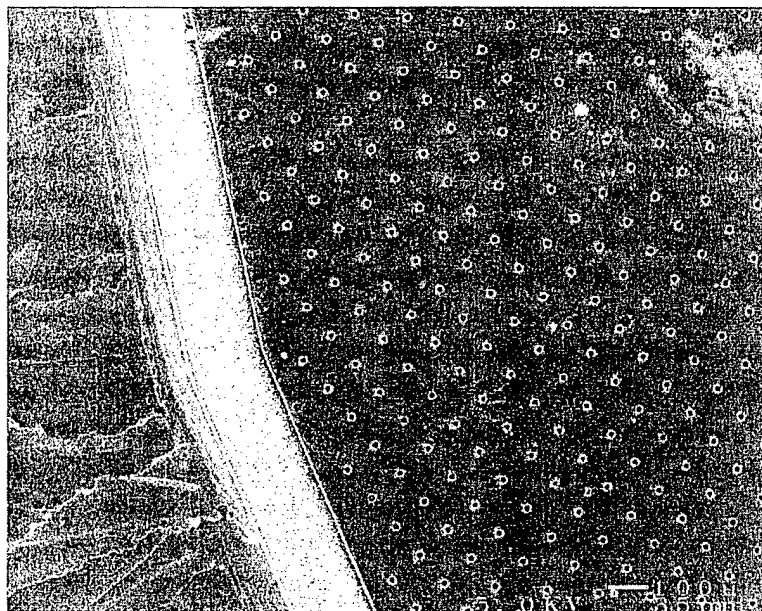
Figure 3: SEM photomicrograph of the etched pattern on a silicon wafer.
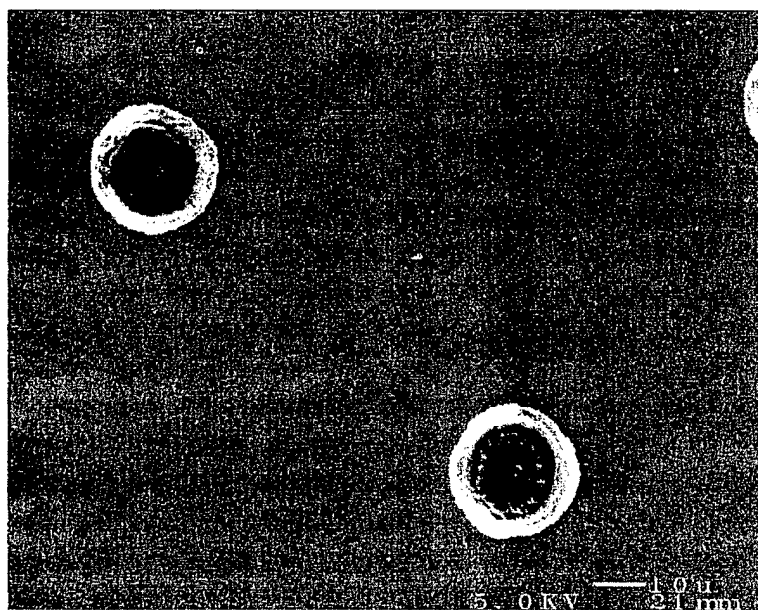

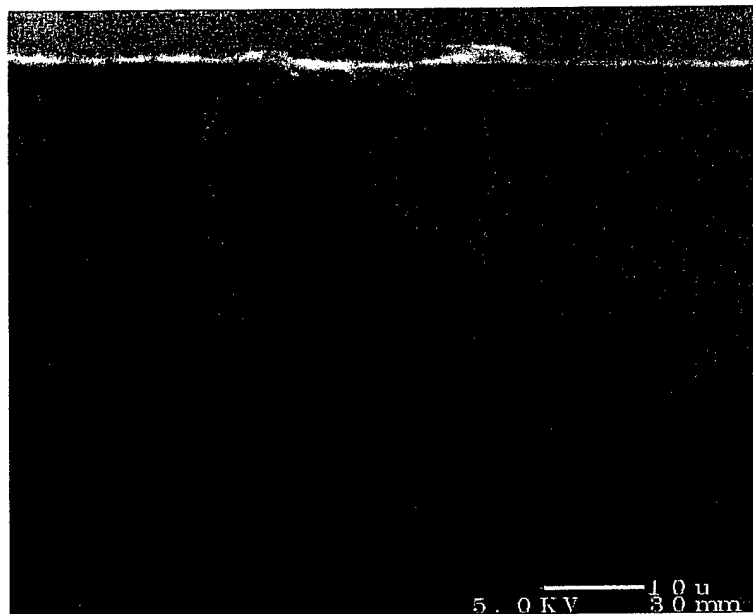**Figure 4:** Top view of two of the holes etched in a silicon wafer.

Figure 5: Cross sectional view of a hole etched into the silicon wafer. Etch time was 60 minutes. The aluminum etch mask has not been stripped, and is visible at the top.

ameter at the top of the hole was about 40 μm. The decrease in longitudinal etch rate with hole depth is expected if it is limited by etchant and product transport. The average transverse etch rate is also significantly smaller in this case as well. The decrease could also be explained by the same mechanism since the wall of the hole being etched is farther from the mask entrance, and the expanded wall area would be expected to reduce the concentration of reactant.

We found that thermal contact between the silicon wafer and the water-cooled holder was an important issue for the lateral etch rate. If the sample was simply clamped at the edges on the copper plate, the lateral etching was much more severe that the results reported here. We used silver paint to hold the wafer on the plate and to provide needed thermal contact. This procedure reduced the lateral etch rate, but a better method would have been desirable.

3 MID-PLASMA CONSTRICTION

For testing in the configuration in which the plasma is constricted in mid-discharge a source of AC power is required. Kunhardt has reported that the optimal frequency is in the 50 – 100 kHz range. In the early stages of research we constructed a high-voltage AC power supply using an old television flyback transformer and a solid state switching circuit. The frequency was variable, covering the range of about 10 – 40 kHz. Output current was limited and the output voltage varied considerably with frequency due to resonance effects. The source was adequate to demonstrate that a glow-like discharge could be produced in He at nearly atmospheric pressure.

For later stages of the work, we used an Advanced Energy Sources (AES) LF5 low-frequency
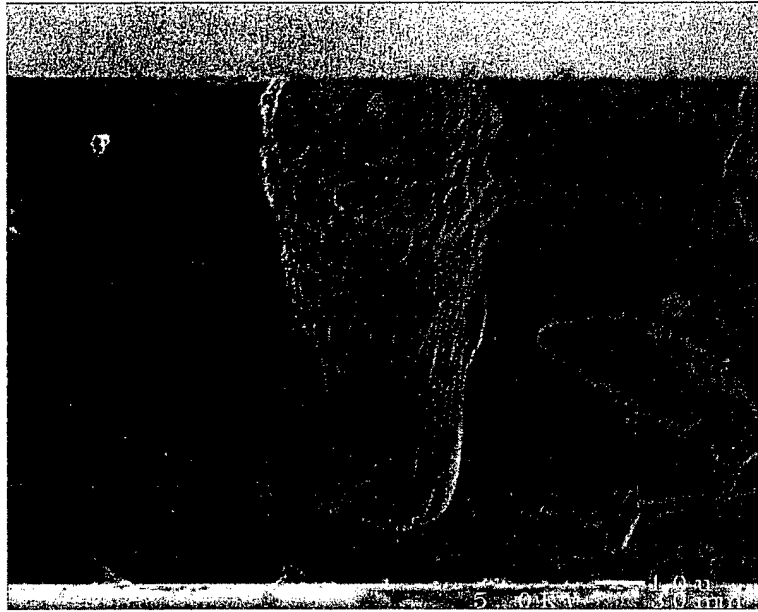
Figure 6: Cross sectional view of a hole etched into the silicon wafer. Etch time was 135 minutes, and the aluminum etch mask has been stripped from the surface.

generator to supply power. It provides up to 500 W of power into 50 Ω, over the frequency range 50 − 400 kHz. For better matching to the discharge, a AES RFPP matching transformer was used. The step-up ratio of this transformer is variable, and it is capable of matching loads of up to 1600 Ω to the 50 Ω output of the generator.

Besides the power source, a cell for holding the sieve or other discharge constrictor was required. Fig. 7 shows a schematic drawing of the cell we used. Pyrex tubing was used for
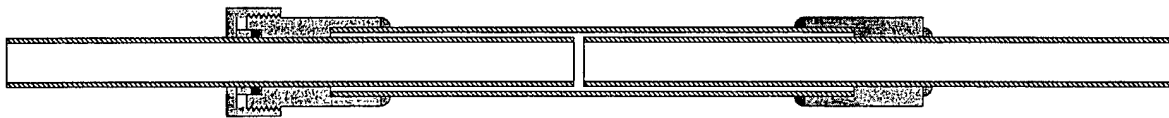

Figure 7: Cross-sectional drawing of the cell we used for the mid-discharge constriction experiments. The cross-hatched sections are pyrex tubing 0.5" and 16 mm in diameter. The solid gray-filled sections are metal. The fillets indicate TorrSeal epoxy used to seal the glass tubing to the metal fixtures. An o-ring seal is used in the fixture on the left to seal to the 0.5" diameter tubing.

electrical insulation and to provide optical access. Tubes with two outside diameters were used. The larger (16 mm OD) provided part of the vacuum envelope. One of the smaller (0.5" OD) tubes was permanently sealed to the metal fixture (as indicated by the TorrSeal fillet). The other 0.5" OD tube was sealed with an o-ring fixture made from a modified Cajon Ultra-Torr fitting. This tube could slide in and out. The sieve or other constrictor was sandwiched between the two 0.5" tubes, with the o-ring-sealed tube adjusted to provide a minimal seal to the constrictor. A Teflon ring or neoprene o-ring could be used for a better seal between either glass tube and

the constrictor, but we did not find it necessary to do so.

Cajon Ultra-Torr fittings were used to connect the 0.5" pyrex tubes to a vacuum pump and to a gas source. The fittings could be used for electrodes as well, or specially-shaped electrodes could be inserted inside the 0.5" tubes and connected to the Cajon fittings with a spring-loaded contact. Besides the fittings themselves, we used points, rings, and planar electrode shapes. We investigated several spacings between these electrodes and the constrictor, varying from about 2 mm from the constrictor to several cm away.

One end of the cell was connected to a mechanical vacuum pump through a valve that could be partly closed to serve as a flow limiter. The other side of the cell was connected to a compressed gas cylinder through a needle valve and a ball-type flowmeter. Pressure gauges were used on both sides of the constrictor. A capacitive-divider voltage monitor was to measure the voltage across the cell, and a low-resistance resistor in series with the current path was used to monitor the current.

Before the discharge starts the gap has a high impedance, dominated by parasitic capacitances. The result is that even with the impedance matching transformer the generator does not see a matched load. As we turned up the generator power in order to raise the gap voltage to the breakdown value, the protection circuitry would typically engage well before breakdown occurred. To avoid this problem, we connected a 2 KΩ power resistor in shunt with the supply, and used the 1600 Ω setting of the matching transformer. With this modification we could turn the generator up to the maximum output power.

3.1 Results

All experiments using the silicon sieves were unsuccessful. The conductivity of the silicon was high enough that it shorted the channels out. Thus, the situation was similar to one with a metal plate placed in mid-gap. This result was expected. Our plan had been to use similar technology to etch holes in a thin quartz wafer. Fluorine-based plasmas etch quartz readily, so the plan was feasible. We did not have sufficient time in the grant period to carry the plan out, however. For this reason, we do not have any data on quartz sieves fabricated in-house.

While waiting for the in-house fabricated sieves, we carried out a number of studies using other constrictors. Fritted glass filters are available commercially, with pore sizes ranging from about 1 μm to more than 100 μm. We used several of these filters as a discharge constrictor. The thickness of each filter disk was about 3.5 mm. In pure He we were able to obtain uniform-appearing, glow-like discharges at pressures up to 760 Torr. The discharge current was small, however, and the the time-dependence of the current exhibited numerous spikes, indicative of an obstructed discharge. Fig. 8 shows an oscillogram of the gap voltage and current for a glass frit with nominal pore diameter 8 μm. The pressure on one side of the frit was 420 Torr, and the pressure on the other is not well known because of a calibration problem, but was about 100 Torr. The dashed line is the voltage across the cell. The peak-to-peak voltage is about 1900 V, and the frequency is about 50 KHz. Except for obvious changes in time scale, the results for higher frequencies were similar.

The current consists of a series of spikes concentrated in regions near maxima in the volt-
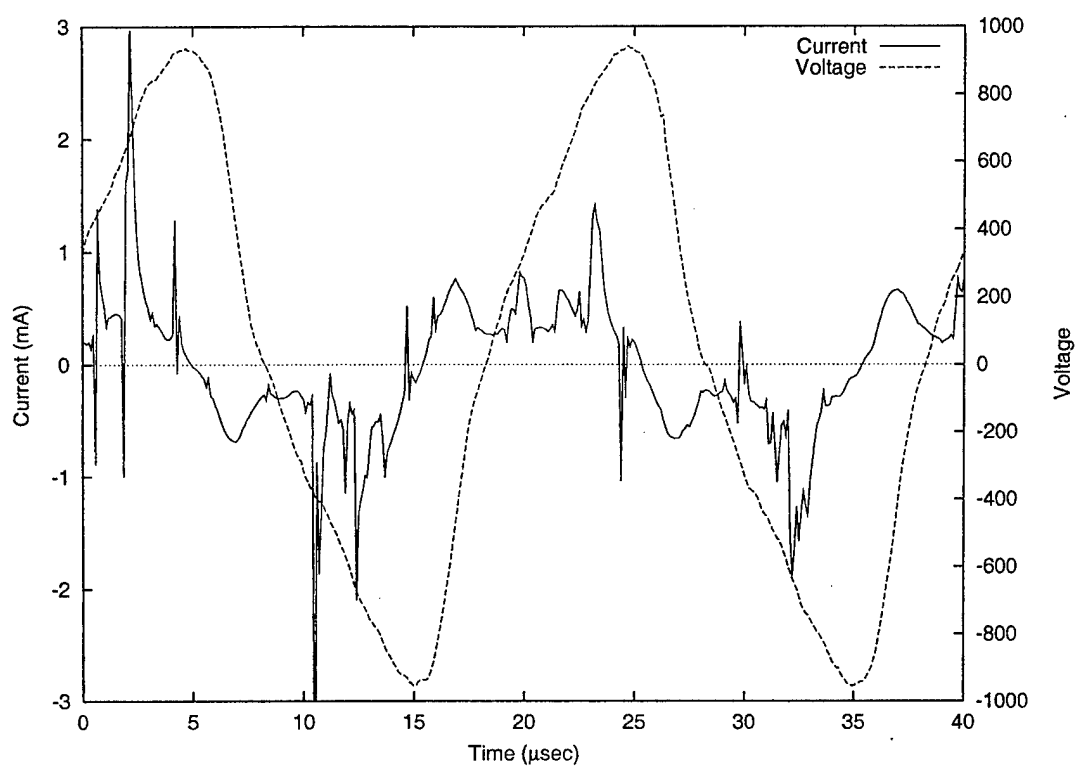
Figure 8: Discharge current and voltage for a glass frit with nominal pore diameter 8 μm in He. The pressure on one side of the frit was 420 Torr, and the pressure on the other side was about 100 Torr.

age magnitude, and on the leading edge of the waveform. These waveforms are similar to those expected from an obstructed discharge, and imply that the discharge we observed at near-atmospheric pressure was of this variety. Although the somewhat open geometry of the cell might be expected to produce resonant ringing effects with such sharp transients, these effects do not seem very important in these data. There is a curious feature in a few of the current spikes, however. In a few cases, such as the first two spikes in Fig. 8, the current first changes in the direction opposite to the applied voltage. We do not understand this feature very well, but speculate it may be due to charging of the insulator from the previous half-cycle.

Besides the spiked current component, there is also a smoother component that roughly follows the voltage waveform. This smoother component can be associated with a more conventional glow or glow-like, persistent discharge plasma. From the magnitude of the component, we can estimate roughly the average electron density in the plasma. For a uniform plasma, the current would be

$$i = nq\mu EA$$

where n is the electron density, q the electronic charge, μ the electronic mobility in 450 Torr He, E the electric field, and A the cross-sectional area. If we approximate the field as being uniform between ≈ 5 cm electrode spacing, and take $A \approx 1$ cm^2, we obtain an estimate of about

$$n \approx 5 \times 10^9 \text{ cm}^{-3}$$

This result underestimates the average density because a significant portion of the applied voltage is probably dropped across the glass frit, but it is unlikely that the actual density exceeded 10^{11} cm^{-3}.

On several occasions, as we increased the voltage across the cell we observed that a hot spot appeared at a point in the glass frit. From the color of the emission, the hot spot appeared to have a temperature exceeding 1000 °C, and the standard sodium emission appeared. Since the average power supplied to the whole discharge is only of the order of one watt, a significant portion of it must have been applied to the frit, implying that most of the applied voltage must have been dropped across the frit.

The appearance of the hot spot raises an interesting possibility for creating higher-density, atmospheric-pressure plasmas. The high temperature in the hot spot would cause substantial electron emission, and localized heating of the gas would increase electron impact ionization rates. This emission could be used to stabilize high-pressure discharges. We did not pursue this possibility because the appearance of a hot spot permanently damaged the pyrex glass frit. Presumably, similar results could have been obtained with a material capable of higher temperature, such as quartz of some ceramics. In the following section, we also discuss briefly the possibility that the physical mechanism responsible for "micro-hollow-cathode" discharges at high pressure may be thermionic emission from the walls of the well, rather than secondary emission from pendular electrons trapped in the well.

4 MICRO-HOLLOW DISCHARGE

We also investigated micro-hollow-cathode discharges as reported by Schoenbach *et al.*, [1] [2] [3], and Frame *et al. et al.*[4]. Although we looked at several configurations, most work was done with the configuration shown in Fig. 9. The structure is built upon an aluminum base. The
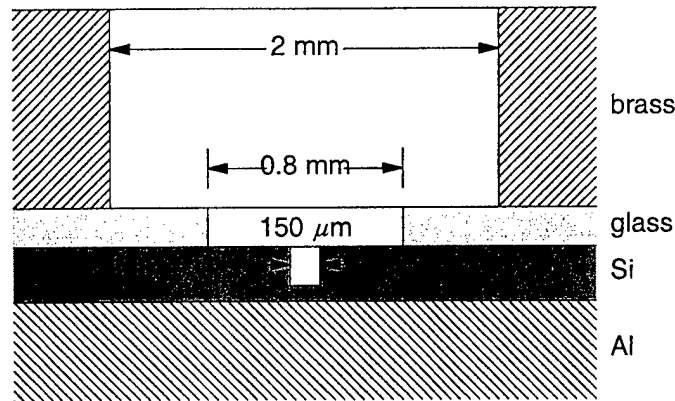

Figure 9: Schematic drawing of the micro-hollow cathode discharge device we investigated.

cathode material is an n-type, 2 Ω–cm silicon wafer, polished on the top surface. The wafer was 0.28 mm thick, and 3.1 cm in diameter. A cavity about 150 μm in diameter and about 200 μm deep was drilled using a a pulsed, 1.06μm, Q-switched Nd:YAG laser. The pulse length was about 10 ns, and the repetition rate was 10 pps. The energy per pulse is not known accurately but was about 10 mJ. A spherical lens was used to focus the beam to a sharp point.

A glass microscope cover slip was used as to insulate the cathode from the anode of the structure. The cover slip had a square shape, 2.2 cm on a side and 0.2 mm thick. A short piece of 0.8 mm diameter drill rod was used with a carborundum slurry to grind a hole through the cover slip. The hole that resulted was about 1 mm diameter. The anode for this device was a brass cylinder 3 mm in thickness and 1.6 cm in outside diameter. A 2 mm diameter hole was drilled through the center to form the cylinder.

The parts were assembled, paying careful attention to alignment of the holes, and the resulting sandwich placed in a plexiglas holder. The layers were held together with a spring-loaded clamp. The assembly was mounted in a stainless steel vacuum chamber which could be evacuated with a mechanical pump. The chamber was equipped with a quartz viewing port, through which the micro-hollow cathode discharge could be observed. A needle valve was used to control the admission of gas into the chamber, and a valve on the mechanical pump was used to control the pressure in the chamber. Experiments were conducted over the pressure range of 20–600 Torr. Using the cathode cavity diameter, this range corresponds to about 0.3 − 9 Torrcm.

Electrically, the aluminum plate was grounded to the stainless steel cell. Connection to the brass anode was made using a high-voltage ceramic feedthrough. A variable DC power supply connected in series with a 27 KΩ resistor for current-limiting. The maximum voltage rating for the power supply was 650 V. Current and voltage were measured using standard DC meters.

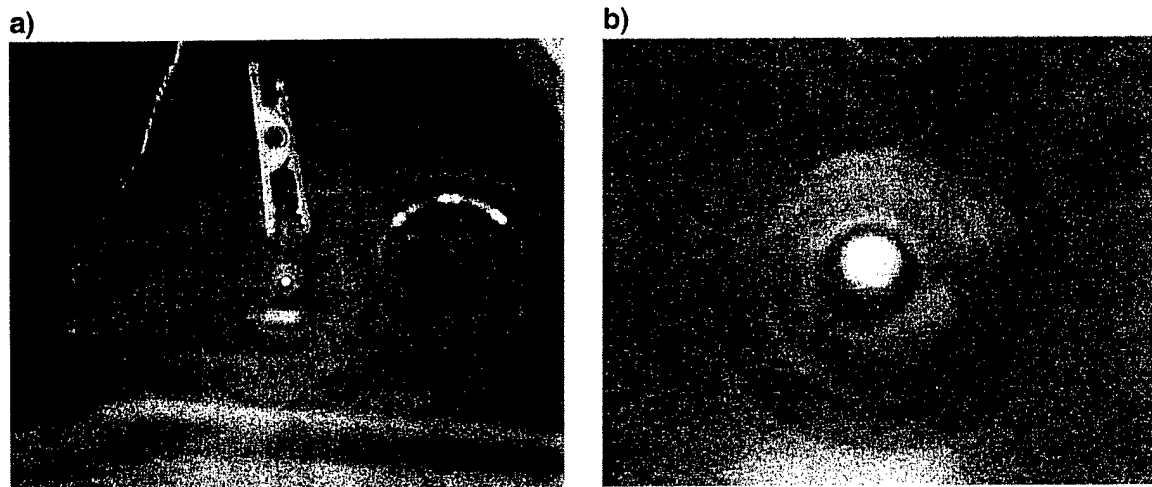Figure 10 shows a photograph of the device in operation. Both an overview of the entire

Figure 10: Photographs showing the micro-hollow discharge device in operation. In (a) the whole device, along with the holder is shown, and (b) shows a close-up view of the discharge. The gas was N_2 at 40 Torr.

device and a close-up view of the discharge are shown. In this case, the fill gas was N_2 at 40 Torr. The small round dot near the center is the discharge filling the hole in the glass cover slip.

At these pressures, the discharge appears uniform within the hole in the insulator. There is additional structure in the region outside this hole which can be seen in photographs without external illumination. Fig. 11 shows two such photographs. Fig. 11(a) shows a discharge in helium at 100 Torr. Besides the bright central spot produced by the discharge within the insulator hole, there is also dimmer halo around the central spot, extended out to the brass anode. This feature is seen more clearly as a faint blue glow against the pink emission from the central spot in color photographs.

Fig. 11(b) shows a discharge in 200 Torr Ar. The uniform central spot is still evident, but in this case the halo surrounding it has developed a set of radial filaments. This constriction into filaments will likely limit the distance over which the glow-like discharge can be maintained.

The role of the central hole in the silicon cathode is of interest. We carried out experiments using devices with the same construction as in Fig. 9, except no hole was drilled in the silicon. For He fills over the pressure range 100–600 Torr we found that breakdown in the device was everywhere filamentary, forming spark channels as is commonly seen in the breakdown of gaps at atmospheric pressure. Thus, it appears that the central hole in the silicon cathode does seem to be playing an important role in the maintenance of a uniform glow, rather than a spark.

We measured the current-voltage characteristics of the cell for several different pressures in Ar, He, and N_2. These data are presented in Figs. 12–14. These results support the contention that the discharge in these devices is based on a hollow-cathode-like mechanism, as proposed by Schoenbach *et al.*. Table I gives the values of pd at the Paschen minimum and the corresponding sparking voltage for the three gases we investigated[6]. Also shown in the table is the pressure corresponding to the Paschen minimum assuming $d = 75\mu$m, half the diameter of the hole in
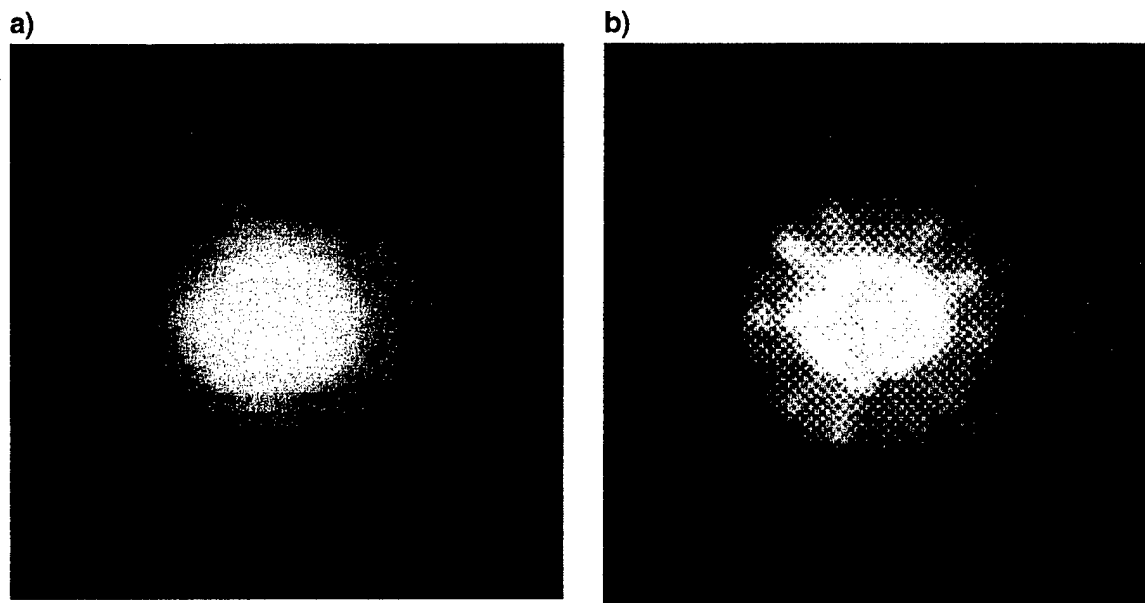
Figure 11: Photographs showing the structure of the discharge outside the hole in the glass insulator, and between this hole and the brass anode. The photo in (a) was taken with helium fill at 100 Torr, that in (b) was taken with Ar at 200 Torr.
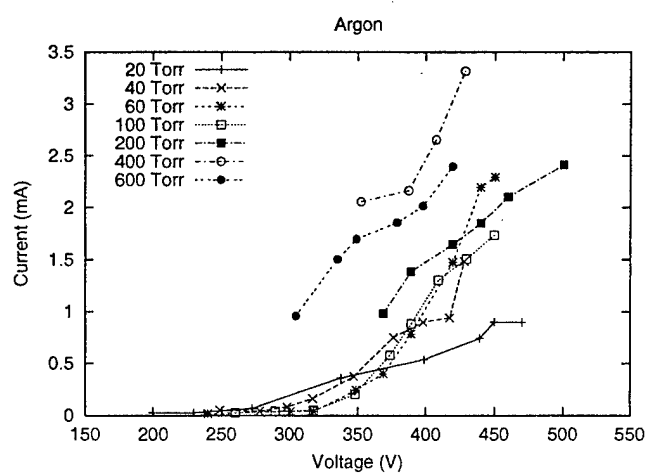

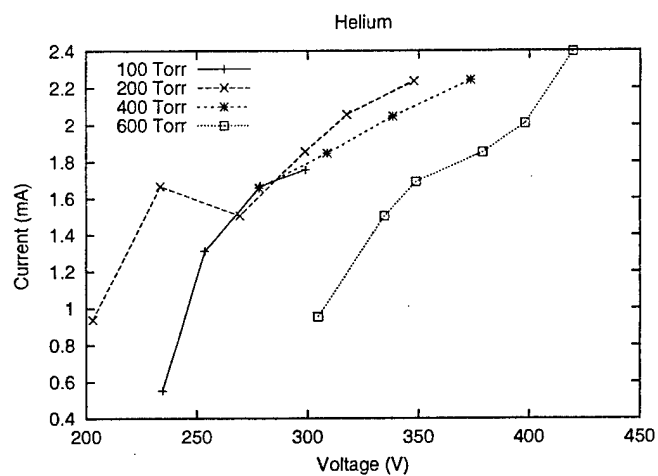**Figure 12:** Current-voltage characteristics for an argon discharge at pressures between 20 and 600 Torr.

14

Helium

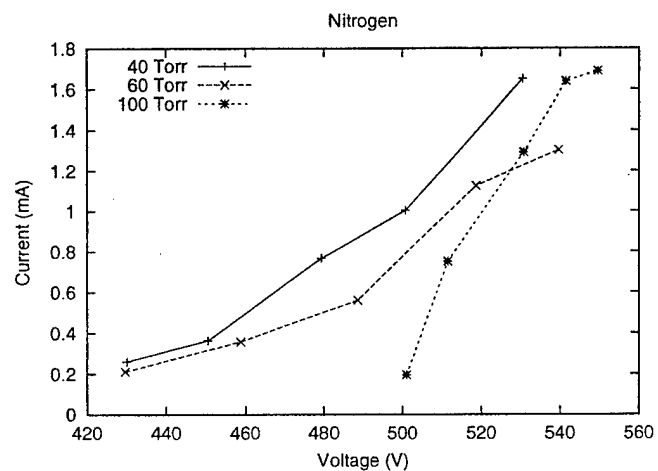**Figure 13:** Current-voltage characteristics for a helium discharge at pressures between 200 and 600 Torr.

Nitrogen

Figure 14: Current-voltage characteristics for an N_2 discharge at pressures between 40 and 100 Torr.

15

Paschen Minima			
Gas	pd_{min} (Torr-cm)	$V_{s\ min}$ (V)	p_{max} (Torr)
Ar	2	180	270
He	4	150	530
N$_2$	1	300	130

Table 1: Values of pd at the Paschen minimum and the corresponding sparking potentials for Ar, He, and N$_2$[6]. Also shown is the pressure for the Paschen minimum assuming $d = 75\ \mu$m.

the silicon cathode.

These data are roughly consistent with the discharge data in Figs. 12–14, and the assumption of a hollow-cathode-like mechanism. A hollow-cathode effect is possible when the cathode-fall region of one side of the well overlaps the cathode fall from the other side. The width of the cathode-fall can be estimated from the pd value at the Paschen minimum by noting that the requirement for the maintenance of a continuous normal glow discharge is the formation of a cathode-fall region. If we require the cathode-falls from the two sides of the cathode to overlap, the smallest that d can be is half the well diameter, $R \approx 75\ \mu$m. Thus, we would expect to be able to induce the discharge up to pressures given approximately by

$$p_{max} = \frac{(pd)_{min}}{R}$$

and this value is given in the last column of Table I.

Direct measurements of the onset of the hollow cathode effect yield similar values. For example, Guntherschulze has measured the current density for a discharge consisting of two parallel plates connected as a cathode, and a large-diameter ring connected as the anode [7]. Measurements were made as function of pd where d is the separation of the two plates, and p is the pressure. For Ar and He, he finds the onset of the hollow-cathode effect to occur at $pd \approx 1.5$ and 3 cm-Torr, respectively.

We did not observe a continuous discharge in N$_2$ for pressures above 100 Torr, consistent with the predicted maximum of 130 Torr. For helium, the predicted maximum pressure is 530 Torr. The highest pressure for which we observed the quasi-uniform discharge in helium was 600 Torr, again remarkably consistent with the prediction.

In argon, the predicted maximum pressure is 270 Torr. We observed operation of our discharge in argon at pressures up to 600 Torr, somewhat above the predicted minimum. There was, however, a marked change in the current-voltage characteristics between 200 and 400 Torr. For pressures between 40 and 100 Torr, the characteristics were very similar. At 200 Torr, however, the voltage to produce a given current decreased slightly, and we did not observe a discharge with current less than about 1 mA. These data are consistent with a change in discharge mode occurring at about 200 Torr, a bit below the predicted maximum pressure of 270 Torr for argon. Fig. 11(b) shows the presence of radial constrictions in the argon discharge at 200 Torr. These constrictions were not present at lower pressure. Similar constrictions were seen in He, starting

16

at 600 Torr. Fig. 15 illustrates the point by showing photos of the helium discharge at 200 and 600 Torr.
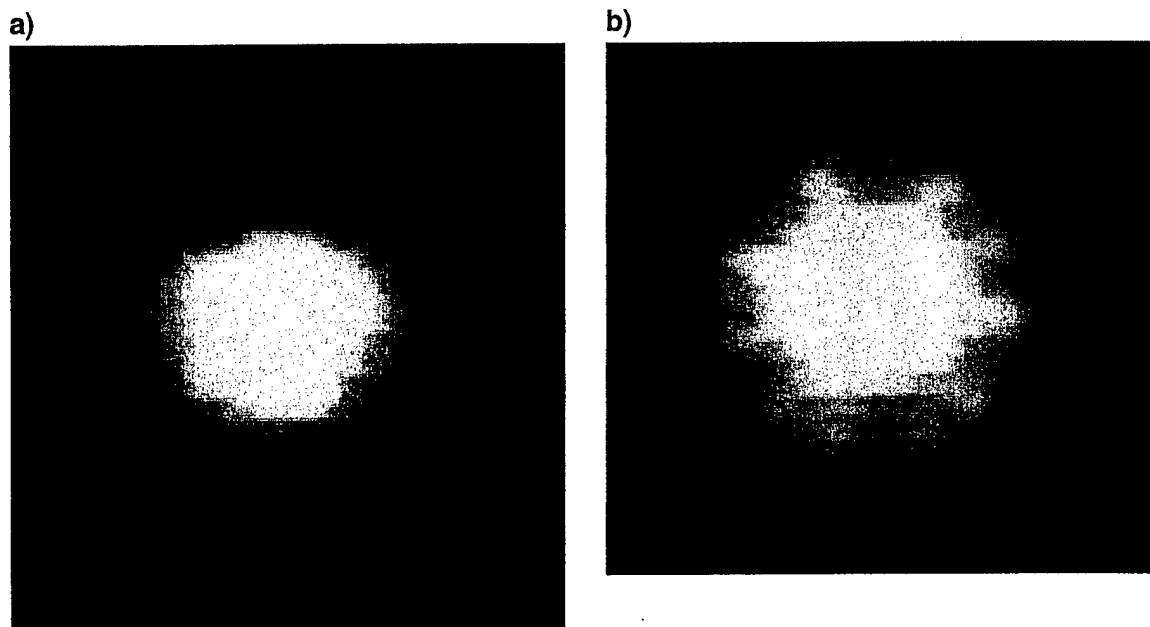
a)

b)

Figure 15: Photographs of the discharge in helium at (a) 200 Torr, and (b) 600 Torr showing the change in apparent discharge mode with pressure.

The cell voltage is also consistent with the minimum sparking voltage at the Paschen minimum. The minimum discharge voltage varies from about 200 V for He to about 300 V for argon, to about 420 V for N_2. These should be compared to the sparking voltages at the Paschen minimum of 150, 180, and 300 V for the three gases, respectively.

An interesting feature of these data is that for a given gas, the characteristic depends only weakly on pressure. This observation is somewhat surprising and suggests that the discharge depends primarily a surface-moderated mechanism, rather than a gas ionization mechanism such as postulated in the hollow-cathode effect. A possible alternative mechanism would be heating of the cathode surface and perhaps the surface of the glass insulator. At temperatures in excess of about 1000 C significant thermionic emission would be expected which would contribute to the electron emission from the cathode. Further, localized heating of the gas would increase electron-impact ionization rates. In such a model, current would be determined primarily by the temperature of the cathode and surrounding gas, which would depend only weakly on gas pressure (assuming the dominant cooling mechanism is heat conduction through the silicon cathode). Such a mechanism would also be consistent with the effects associated with the appearance of a hot spot in the glass frit as discussed in Section 3.

References

[1] K. H. Schoenbach, R. Verhappen, T. Tessnow, F. E. Peterkin and W. W. Byszewski, Appl. Phys. Lett. 68 (1996) 13.

[2] R. H. Stark and K. H. Schoenbach, Appl. Phys. Lett. 74 (1999) 3770.

[3] _____, J. Appl. Phys. 85 (1999) 2075.

[4] J. W. Frame, D. J. Wheeler, T. A. DeTemple and J. G. Eden, Appl. Phys. Lett. 71 (1997) 1165.

[5] D. L. Flamm, "Plasma Chemistry, Basic Processes, and PECVD,"in *Plasma Processing of Semiconductors*, P. F. Williams, Ed. Dordrecht: Kluwer, p. 61, 1997.

[6] M. J. Schönhuber, IEEE Trans. Power App. and Sys. PAS-88 (1969) 100.

[7] A. von Engel, in *Ionized Gases*. London: Oxford, p. 237, 1965, Original article: A. Guntherschulze, Z. tech. Phys. **11**, 49 (1930)..